A *TESS* search for donor-star pulsations in high-mass X-ray binaries

Gavin Ramsay [iD],[1][*] Pasi Hakala[2] and Philip A. Charles[3]

[1]*Armagh Observatory & Planetarium, College Hill, Armagh BT61 9DG, UK*
[2]*Finnish Centre for Astronomy with ESO (FINCA), Quantum, University of Turku, FI-20014 Turku, Finland*
[3]*School of Physics and Astronomy, University of Southampton, Highfield, Southampton SO17 1BJ, UK*

ABSTRACT

Ground-based optical photometry of the counterparts of high-mass X-ray binaries (HMXBs) has revealed the presence of periodic modulations on time-scales of $\sim$0.3–0.5 d. More recent space-based observations (*CoRoT* and *TESS*) of OB and Be stars have shown that pulsations caused by p and g modes are common in early-type stars. We have therefore undertaken a systematic search for variability in the optical counterparts of 23 HMXBs (mostly neutron star systems, but including one black hole, Cyg X-1) using *TESS* data primarily in 2 min cadence mode. After removing the orbital period modulation in four systems, we find that all 23 sources show evidence for quasi-periodic variability on periods shorter than $\sim$1 d. We compare their power spectra with those from observations of other OB- and Be-type stars. In two systems, V725 Tau and HD 249179 (which may not be an HMXB), we find evidence for an outburst, the former being simultaneous with an X-ray flare. We search for changes in the power spectra over the outburst duration and compare them with outbursts seen in other Be systems.

Key words: circumstellar matter – stars: early-type – stars: emission-line, Be – stars: oscillations – X-rays: binaries.

1 INTRODUCTION

High-mass X-ray binaries (HMXBs) are intense X-ray sources consisting of a compact star, either a neutron star (NS) or a black hole (BH), and a giant or supergiant companion star that is close to filling its Roche lobe. Accretion on to the primary takes place in the form of an accretion disc and/or via a stellar wind from the hot companion. They have orbital periods ranging from days to months, and many have a high binary eccentricity that can cause short-duration X-ray outbursts on the orbital cycle as the companion star passes through periastron (Type I outbursts). Longer duration outbursts lasting several orbital cycles (Type II outbursts) are seen less frequently (see Okazaki & Negueruela 2001 for an overview of the outburst models). For a detailed review of HMXBs, see Lewin & van der Klis (2006).

The optical light curves of HMXBs over an interval of days and weeks can be complex, and are a combination of the ellipsoidal modulation of the secondary star with the effect of a tilted and precessing accretion disc (e.g. Gerend & Boynton 1976). On shorter time-scales, observations by Gutierrez-Soto et al. (2011) of two HMXBs revealed short-period modulations that were identified as being due to non-radial pulsations from the companion star in V635 Cas (0.30 d) and GSC 03588−00834 (0.45 d). Observations using wide-field imaging surveys, such as OGLE IV, have allowed the discovery of short-period photometric modulations in other HMXBs (e.g. Schmidtke et al. 2014, 2016, 2019). If the nature of these periodic signals can be effectively modelled, they can give insight into the internal structure of the companion star in HMXBs.

The discovery of pulsations from the secondary star in some HMXBs is not especially surprising since they are OB stars with spectral types ranging from supergiants (e.g. HDE 226868, the optical companion to Cyg X-1) to dwarfs (e.g. V490 Cep), which have previously shown pulsations. The slowly pulsating B-type stars (SPBs) display high-order g modes (with periods $\geq$6 h), while the β Cep stars can show lower order p modes (periods $\sim$1–8 h) and g modes (see De Cat et al. 2010 for a review of observations made using *CoRoT*). More recently, Labadie-Bartz et al. (2022) made an analysis of 432 classical Be stars observed by *TESS* during its first year of operation. Almost all of these stars showed significant variability and their power spectra could be classified, with 85 per cent showing closely spaced frequencies in their power spectra.

The launch of satellites such as *CoRoT* and *TESS* has provided a golden opportunity to search for pulsations in stars of all types, including X-ray binaries. Although none were known in the original 115 deg^2 *Kepler* field (Borucki et al. 2010), the prototypical LMXB Sco X-1 was observed when *Kepler* was repurposed as *K2* with fields along the ecliptic being observed for 2 month blocks (see Hakala et al. 2015; Scaringi et al. 2015; Hynes et al. 2016). *TESS* was launched in 2018 April, and although it does not go as deep as *Kepler*, it does provide high signal-to-noise photometry of sources down to $V \sim$ 13–14 (see Ricker et al. 2015 for more details). In its initial 2 yr mission, it observed $\sim$3/4 of the whole sky, with a gap along the ecliptic plane and an additional section of the Northern hemisphere. Given that some HMXBs are optically bright, this provides an opportunity to search for short-period pulsations, of the type identified by Gutierrez-Soto et al. (2011) and Schmidtke et al. (2014, 2016, 2019).

In this paper, we present observations of the optical light curve of 23 HMXBs and identify those that show evidence for short periodic, likely pulsation, variations. We have not attempted to do a full frequency analysis of the light curves, but rather determine how

[*] E-mail: Gavin.Ramsay@armagh.ac.uk

common pulsations are in the donor stars of HMXBs. Further, we identify two systems that show an optical outburst, one of which is simultaneous with a low-energy X-ray outburst. We compare these findings with observations of other Be stars.

2 THE HMXB SAMPLE

As we are searching for periodic variability on a time-scale of $\lesssim 1$ d, we restrict our sample to include HMXBs that have *TESS* 2 min cadence data or a calibrated light curve made using full-frame image data (see Section 3 for further details). We cross-matched all stars observed in Cycles 1–4[1] with the HMXB catalogue of Liu et al. (2006), finding 23 sources that are detailed in Table 1. Four of our sample have supergiant donor stars, while more than half the sample has Be-type donors. Although HD 49798 is classed as an HMXB in Liu et al. (2006), this appears to be an sdO/WD binary and is therefore not included in this study. HD 141926 is included in the catalogue of candidate Herbig Ae/Be stars (Vieira et al. 2003) and hence its evolutionary state will differ from other stars in this sample. In Section 4.2, we note that HD 249179 might not be an HMXB: however, for reasons outlined there, we decided to retain this source as part of our study.

For further insight as to the nature of the donor stars in these 23 HMXBs, we use the *Gaia* EDR3 parallaxes (Gaia Collaboration 2021) to infer their distances.[2] In practice, we use a routine in the STILTS package (Taylor 2006) and use a scale length $L = 1.35$ kpc, which is appropriate for stellar populations in the Milky Way in general. From these distances, we determine their absolute magnitudes in the *Gaia* G band (a very broad optical filter), M_G, using the mean *Gaia* G magnitude. The other key observables are the blue (BP) and red (RP) filtered magnitudes, which are derived from the *Gaia* prism data. We then deredden the (BP − RP) and M_G values using the 3D dust maps derived from Pan-STARRS1 data (Green et al. 2019) and the relationship between $E(B − V)$, $E(BP − RP)$, A_G, and $E(BP − RP)$ outlined in Andrae et al. (2018). For those stars just off the edge of the Pan-STARRS1 field of view (stars with $\delta < −30°$), we take the nearest reddening distance relationship. We include the distances to our targets and M_{G0} and (BP − RP)$_0$ in Table 1.

The nearest HMXB in our sample is μ^2 Cru, which is only 120 pc distant (we note that although μ^2 Cru is bright, $T_{mag} = 5.3$, there is another star 35.3 arcsec distant, which has $T_{mag} = 4.2$, so some contamination in the light curve will be present). In contrast, V490 Cep (1H 2138+579) is ∼9 kpc distant, although with a large uncertainty. We show the dereddened M_{G0} and (BP − RP)$_0$ values for our sample in Fig. 1, where the size of the symbols reflects the binary orbital period (if known). To give context, we also show the apparent M_G and (BP − RP) values for stars within 50 pc and assume that they show negligible reddening. What is immediately striking is the spread in position of our sample HMXBs in the *Gaia* Hertzsprung-Russell Diagram (HRD). Cyg X-1, the one system that we know has a BH primary, is near the upper part of the distribution.

---

[1]The sources in this paper were on the 2 min cadence list, thanks to their inclusion on the following Guest Investigator programmes: G011060/PI Paunzen; G011155/PI Huber; G011204/PI Pepper; G011224/PI Redfield; G011268/PI Scaringi; G011281/PI Silvotti; G022020/PI Dorn-Wallenstein; G022062/PI Prsa; G022071/PI Scaringi; G022172/PI Labadie-Bartz; G022184/PI Coley; G03156/PI Pope; G03186/PI Labadie-Bartz; G03221/PI Barlow; G04067/PI Wisniewski; G04074/PI Bowman; and G04103/PI Huber.

[2]Following the guidelines of Bailer-Jones (2015), Astraatmadja & Bailer-Jones (2016), and Gaia Collaboration (2018), which are based on a Bayesian approach.

Those sources close to Cyg X-1 are V662 Cas (an NS primary with a very slow rotation period of 2.78 h; Hall et al. 2000) and CI Cam, the nature of whose primary remains controversial.

3 THE *TESS* DATA

TESS, launched on 2018 April 18, has four telescopes, each with an aperture of 10.5 cm that cover a $24° \times 90°$ sector of sky for ∼27 d. In the prime mission, the majority of the sky was observed apart from a strip along the ecliptic plane. In the first year of the extended mission, the southern ecliptic hemisphere was observed for a second time, while in the second year those regions not observed in the prime mission were covered with a second observation of northern fields.

The *TESS* camera detectors have 21 arcsec × 21 arcsec pixels, with the point spread function covering more than 2×2 pixels, which can make blending an issue especially in crowded fields. For the first two years, ∼20 000 predefined targets were observed in each sector with a 2 min cadence, with a 20 s cadence being introduced in year 3. In years 1 and 2, full-frame images with a cadence of 30 min are available, with the cadence increasing to 10 min in year 3. All of our targets, with the exception of HD 109857 (which has 30 min cadence in sectors 11–12 and 10 min in sectors 38–39), were observed in 2 min cadence.

We downloaded the calibrated light curves with 2 min cadence of our targets from the Mikulski Archive for Space Telescopes (MAST) data archive.[3] We used the data values for PDCSAP_FLUX, which are the Simple Aperture Photometry values, SAP_FLUX, after the removal of systematic trends common to all stars on that chip. Each photometric point is assigned a QUALITY flag, which indicates if the data have been compromised to some degree by instrumental effects. For HD 109857, we obtained calibrated light curves from full-frame images using the TESS-SPOC pipeline (Caldwell et al. 2020), again from the MAST data archive.[4] We removed those points that did not have QUALITY = 0 and normalized each light curve by dividing the flux of each point by the mean flux of the star in that sector.

As an example of the light curves obtained by *TESS*, we show in Fig. 2 V635 Cas, which has a clear short-period modulation with the same period (0.3 d) as found by Gutierrez-Soto et al. (2011), and HDE 226868 (the optical counterpart to Cyg X-1). The latter displays the signature of the 5.6 d orbital period through the well-known ellipsoidal modulation of the donor star (hence its appearance as peaks every 2.8 d). Even though Cyg X-1 is an extremely luminous ($\geq 10^{37}$ erg s^{-1}) X-ray source, the donor is an OB I star, so the effects of X-ray heating are small. (As a benefit to the reader we show one sector of *TESS* data for each of our targets in Figs A1–A4.)

Four sources showed evidence of orbital modulations (GP Vel, V884 Sco, HDE 226868, and V662 Cas). We detrended these light curves using the flatten routine in the LIGHTKURVE PYTHON package (Lightkurve Collaboration 2018) to search for shorter period variability. After some trial and error, we chose a window length for the filter of 1 d: We acknowledge that the resulting detrended light curves could contain features that are a result of this choice of window length. Nevertheless, we show in the lower panel of Fig. 2 the detrended light curve of HDE 226868, which reveals significant short-period variability in the light curve (we show the normalized and detrended light curves for GP Vel, B884 Sco, and V662 Cas in Fig. B1). In sector 44, X Per shows a prominent sinusoidal variation on a time-scale of ∼15 d (see Fig. A3), which is much shorter than

---

[3]https://archive.stsci.edu/tess/
[4]https://archive.stsci.edu/hlsp/tess-spoc

Table 1. Properties of HMXBs observed by *TESS* in 2 min cadence mode.

Name	Other name	TIC	T_{mag}^a	Sectors	Spectral type	P_{orb} (d)	Distance^b (kpc)	M_{G0}^c	$(BP - RP)_0^c$	Primary	Power spectra type
GP Vel	Vela X-1	191450569	6.3	8, 9	B0.5 Ib	8.96	$2.0^{+0.1}_{-0.1}$	−5.8	0.2	NS	Mid
Hen 3-640	1A 1118−615	468095832	10.7	10, 37, 38	O9.5Ve	24.0	$3.0^{+0.2}_{-0.1}$	−2.0	0.9	NS	Mid/low
V801 Cen	2S 1145−619	324268119	8.7	10, 37, 38	B0.2IIIe	187.5	$2.1^{+0.1}_{-0.1}$	−4.0	0.0	NS	Mid
BZ Cru	1H 1249−637	433936219	5.2	11, 37, 38	B0.5IIIe	–	$0.44^{+0.03}_{-0.02}$	−3.4	0.4	NS	Mid
μ^2 Cru	1H 1255−567	261862960	5.3	11, 37, 38	B5Ve	–	$0.121^{+0.003}_{-0.003}$	−0.4	−0.2		Mid
HD 141926	1H 1555−552	84513533	8.0	12, 39	B2IIIn		$1.4^{+0.1}_{-0.1}$	−2.7	0.5		Isolated
V884 Sco	4U 1700−37	347468930	6.1	12	O6.5Iaf	3.41	$1.6^{+0.2}_{-0.1}$	−5.3	0.1		Mid
HDE 226868	Cyg X-1	102604645	7.9	14	O9.7 Iab	5.6	$2.2^{+0.2}_{-0.1}$	−4.3	0.7	BH	Mid
GSC 03588−00834	SAX J2103.5+4545	273066197	13.0	16	B0Ve	12.68	$7.4^{+1.5}_{-0.9}$	−2.3	0.7	NS	Mid
V490 Cep	1H 2138+579	341320747	13.0	16, 17	B1-B2Ve	–	$9.0^{+2.1}_{-1.2}$	−2.8	0.6	NS	Mid/low
BD+53 2790	4U 2206+543	328546890	9.6	16, 17	O9.5Ve	9.57	$3.3^{+0.2}_{-0.2}$	−4.1	−0.2	NS	Mid
V662 Cas	2S 0114+650	54469882	9.8	18, 24, 25	B0.5Ib	11.6	$5.1^{+0.5}_{-0.4}$	−4.5	0.8	NS	Isolated
V635 Cas	4U 0115+634	54527515	13.3	18, 24, 25	B0.2Ve	24.3	$7.0^{+1.8}_{-1.0}$	−1.7	1.3	NS	Mid
BQ Cam	EXO 0331+530	354185144	13.0	18, 19	O8.5Ve	34.25	$7.0^{+2.2}_{-1.1}$	−1.8	1.5	NS	Mid
X Per	4U 0352+309	94471007	6.0	18, 43, 44	B0Ve	250.3	$0.61^{+0.03}_{-0.02}$	−3.2	0.3	NS	Isolated
CI Cam	XTE J0421+560	418090700	9.9	19	sgB[e]	19.41	$4.7^{+0.7}_{-0.5}$	−4.0	0.9		Isolated
LS V +44 17	RX J0440.9+4431	410336237	10.0	19	B0.2Ve	150.0	$2.6^{+0.2}_{-0.1}$	−2.8	0.5	NS	Mid
V420 Aur	EXO 051910+3737.7	143681075	7.0	19	B0IVpe		$1.4^{+0.1}_{-0.1}$	−4.2	0.1		Isolated
HD 109857^d	1H 1253−761	360632151	6.5	11, 12, 38, 39	B8V		$0.21^{+0.02}_{-0.02}$	−0.3	0.1		Isolated
V725 Tau	1A 0535+262	75078662	8.2	43–45	O9/B0III/Ve	111.0	$1.91^{+0.16}_{-0.12}$	−3.7	0.5	NS	Isolated
IGR J06074+2205		45116246	11.8	43, 44	B0.5Ve		$6.9^{+1.9}_{-1.0}$	−3.8	−0.1		Isolated
BD+47 3129	RX J2030.5+4751	187940144	8.7	41	B0.5V-IIIe		$2.39^{+0.17}_{-0.13}$	−3.9	0.2		Isolated
HD 249179	4U 0548+29	78499882	9.2	43–45	B5ne		$1.68^{+0.16}_{-0.12}$	−2.0	−0.3		Mid

^{a}Magnitude in the *TESS* pass-band.
^{b}From *Gaia* EDR3.
^{c}Dereddened.
^{d}Data taken in 30 min cadence.

Table 2. The principal periods determined for our targets on a sector-by-sector basis (indicated by the square brackets) using the LS periodogram.

Object	Periods (d)
GP Vel	[8] 0.521 [9] 0.656
Hen 3-640	[10] 1.066 [37] 3.06 [38] 3.05, 1.072
V801 Cen	[10] 0.665, 0.357, 0.464 [37] 0.358, 0.463, 0.661 [38] 0.463, 0.358, 0.375
BZ Cru	[11] 0.339, 0.104, 0.969 [37] 0.725, 0.637, 0.694 [38] 0.636, 0.339, 0.725
μ^2 Cru	[11] 1.614, 0.935, 0.989, 0.336 [37] 0.918, 1.005, 0.337, 1.066 [38] 1.598, 0.930, 0.337, 0.893
HD 141926	[12] 0.904, 0.953, 0.419 [39] 0.904, 0.407, 0.415
V884 Sco	[12] 0.729, 0.763, 0.614
HDE 226868	[14] 0.661, 0.597, 0.578
GSC 03588−00834	[16] 0.448, 0.102
V490 Cep	[16] 1.970, 0.538 [17] 1.963, 1.772
BD+53 2790	[16] 1.120, 0.981, 0.647 [17] 0.998, 0.834, 0.791
V662 Cas	[18] 0.497, 0.352, 0.572 [24] 0.687, 0.741, 0.791 [25] 0.594, 0.613, 0.578
V635 Cas	[18] 0.3003 [24] 0.3003 [25] 0.3010
BQ Cam	[18] 0.419, 0.755 [19] 0.420, 0.756
X Per	[18] 0.574, 0.277 [43] 0.575, 0.277 [44] 0.277, 0.529
CI Cam	[19] 0.406
LS V +44 17	[19] 0.385, 0.460
V420 Aur	[19] 0.672, 1.446
HD 109857	[11] 0.568, 0.284 [12] 0.569, 0.285 [38] 0.571, 0.454, 0.285 [39] 0.570, 0.284, 0.453
V725 Tau	[43] 0.468 [44] 0.469 [45] 0.468
IGR J06074+2205	[43] 0.434 [44] 0.435
BD+47 3129	[41] 1.225
HD 249179	[43] 0.283 [44] 0.490, 0.283 [45] 0.282
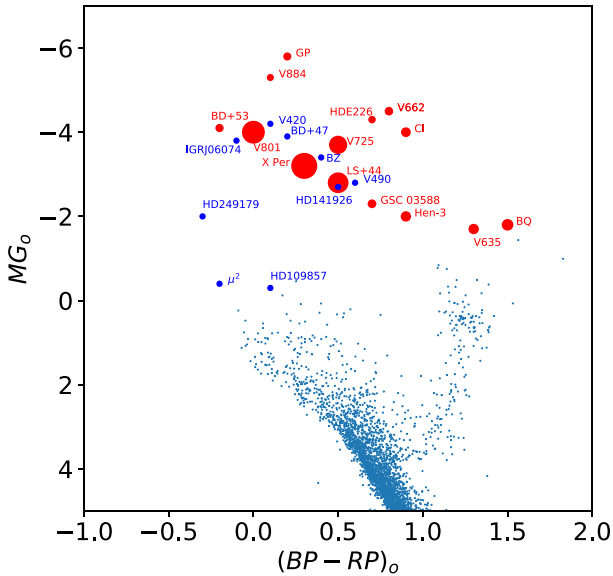
Figure 1. The *Gaia* HRD [(BP − RP)$_0$, M_{G0}] where the blue dots represent stars within 50 pc of the Sun and we assume they have negligible reddening. The HMXBs in our sample are shown as circles with a shortening of their name and are dereddened as outlined in the main text. Blue circles indicate those with unknown $P_{\rm orb}$, while the size of the red circles is proportional to $P_{\rm orb}$.

its orbital period of 250 d. We also removed the 15 d trend in X Per to search for shorter period variability.

To search for periodic variations in the light curves, we used the generalized Lomb–Scargle (LS) periodogram (Press et al 1992; Zechmeister & Kürster 2009), obtaining a power spectrum for each sector the star was observed. We show the power spectra obtained for each source in Figs 3–5 with the periods of the most prominent peaks shown in Table 2 on a sector-by-sector basis.

In their study of 432 classical Be stars made using *TESS* data, Labadie-Bartz et al. (2022) classified them based on their power spectra. The classifications include low-frequency (>2 d) signals that dominate and are typical of g-mode pulsations; frequency groups in the mid-frequency range (0.16–2 d) closely spaced groups (p and g modes); high-frequency (0.06–0.16 d) signals dominate (p and g modes); and single isolated frequencies – sources can have more than one classification. We made an assessment of the power spectra shown in Figs 3–5 and classified them based on the criteria of Labadie-Bartz et al. (2022). We find that 13/23 (57 per cent) have mid-frequency spectra, 8/23 (35 per cent) have isolated spectra, and 2/23 (9 per cent) show both mid- and low-frequency spectra. In comparison, Labadie-Bartz et al. (2022) find that 32 per cent of Be stars show isolated frequencies and 85 per cent show frequency groups. Hen 3-640 was included in both this study and that of Labadie-Bartz et al. (2022), with us classifying the power spectra as mid/low and Labadie-Bartz et al. (2022) indicating it shows low-frequency trends and isolated signals (including at high frequencies). Given the element of uncertainty in classifying the power spectra of the HMXB in our sample, the light curves analysed here appear to be broadly similar to the classical Be stars reported in Labadie-Bartz et al. (2022).

In Fig. 6, we show the same *Gaia* HRD as we showed in Fig. 1 but here we have colour coded the sources depending on their classification shown in Table 1. There appears to be no separation between sources showing mid-frequency groups, isolated signals, and those showing mid- and low-frequency signals.

We now comment on some specific sources. GSC 03588−00834 (SAX J2103+4545) shows two eclipses in its *TESS* light curve separated by 16.6 d. Given that this is longer than the orbital period, this suggests that one of two relatively bright stars ($G = 13.9$, $G = 14.3$) within 21 arcsec (the *TESS* pixel size) is the source of the eclipses. The light curve also shows evidence of two dip-like features, which may be related to the orbital period. Using a weighted
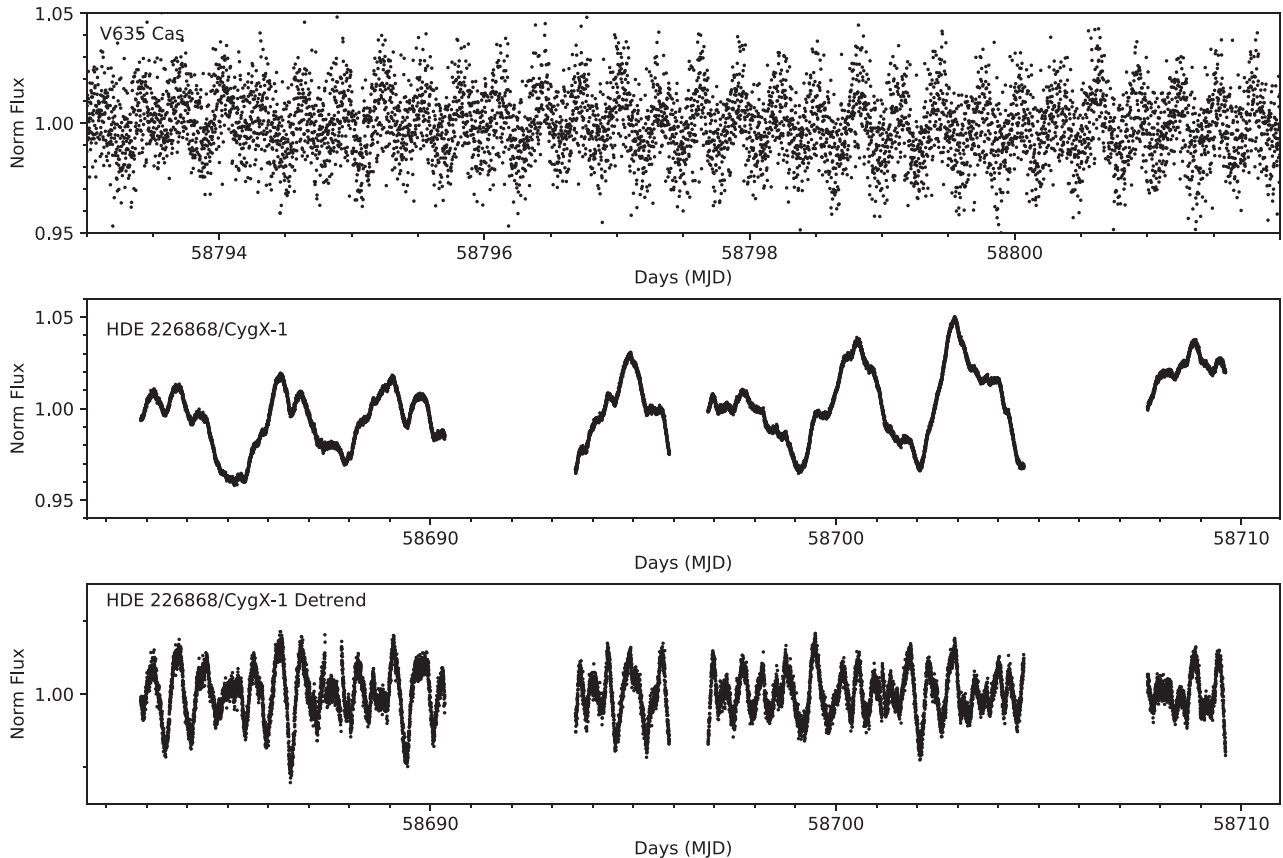
Figure 2. Upper panel: a 9 d section of *TESS* 2 min cadence data of V635 Cas from sector 18. There is a clear modulation on a period of 0.30 d. Middle panel: the *TESS* 2 min cadence data of HDE 226868 (Cyg X-1) obtained in sector 14. A high-amplitude modulation is seen on the orbital period (5.6 d) and half the orbital period. Lower panel: the light curve of HDE 226868 detrended to remove the signature of the orbital period.

wavelet Z-transform (Foster 1996) to search for evidence of short-period variations, we found evidence for a period that drifts in the three sectors of data between 0.33 and 0.45 d, which is similar to the period reported by Gutierrez-Soto et al. (2011). However, once we take into account the dilution of the two spatially nearby stars, this increases to 1.2 per cent. We conclude that it is likely that a quasi-periodic signal on a time-scale similar to that reported by Gutierrez-Soto et al. (2011) is present at times in GSC 03588−00834.

We noted earlier that X Per shows a modulation on a time-scale of ∼15 d in sector 44 whose signature we removed before obtaining an LS power spectrum. In Fig. 4 we see that power is concentrated at periods near 0.50–0.55 d in sectors 18 and 43, but in sector 44 the peak in the power spectrum is shifted to an isolated peak at ∼0.3 d (there is no evidence for an X-ray outburst at this time). In Fig. 3 we show the power spectra of Hen 3-640: In sector 10, peaks are seen between periods of 0.5 and 1.1 d, but in sectors 37 and 38, there is a clear modulation in a period of ∼3 d. Similarly, in Fig. 3 we find that BZ Cru shows enhanced power between 0.6 and 0.8 d in sectors 37 and 38 compared to sector 11. For two sources, V725 Tau and HD 249179, we discuss their power spectra in greater detail in the next Section.

4 OUTBURSTS

TESS has been used to observe supernovae prior to their detection in ground-based transient surveys (e.g. Fausnaugh et al. 2021) and also serendipitous outbursts of previously known cataclysmic variables

(e.g. Court et al. 2019). Moreover, outbursts have been seen in many classical Be stars. We therefore manually searched the *TESS* light curves in our sample for any evidence of outbursts. We found outbursts in two of them: V725 Tau and HD 249179.

4.1 V725 Tau

V725 Tau (1A 0535+262/HD 245770) is a prototypical transient X-ray pulsar that has been observed to show many X-ray outbursts, including a recent giant outburst (peaking at 1.2×10^{38} erg s^{-1}) in 2020 November (e.g. Kong et al. 2021). Since then, observations made using Monitor of All-sky X-ray Image (MAXI) showed a weaker outburst around 2021 June 20 (the field was not being observed by *TESS*) and an even weaker X-ray outburst a few months later, starting on October 13 (MJD = 59500). In Fig. 7 (left-hand panels), we show the simultaneous *TESS* and X-ray (MAXI) light curves of V725 Tau during this much weaker outburst. The increase in optical flux suggests an outburst amplitude of ∼0.2 mag (there are no significant issues of dilution from nearby bright stars).

Fig. 7 indicates that there was a clear periodic (∼0.5 d) signal in all three sectors (43–45) of *TESS* data. To investigate this further, we detrended each of these sectors so as to remove the large outburst variation and show the resulting light curve in Fig. C1: It appears like a typical multiperiodic pulsation where modes come and go on a quasi-period of ∼6.4 d, causing a change in the amplitude of the main pulsation. We applied a shifted time window version of the epoch folding periodogram (Davies 1990) to search for the
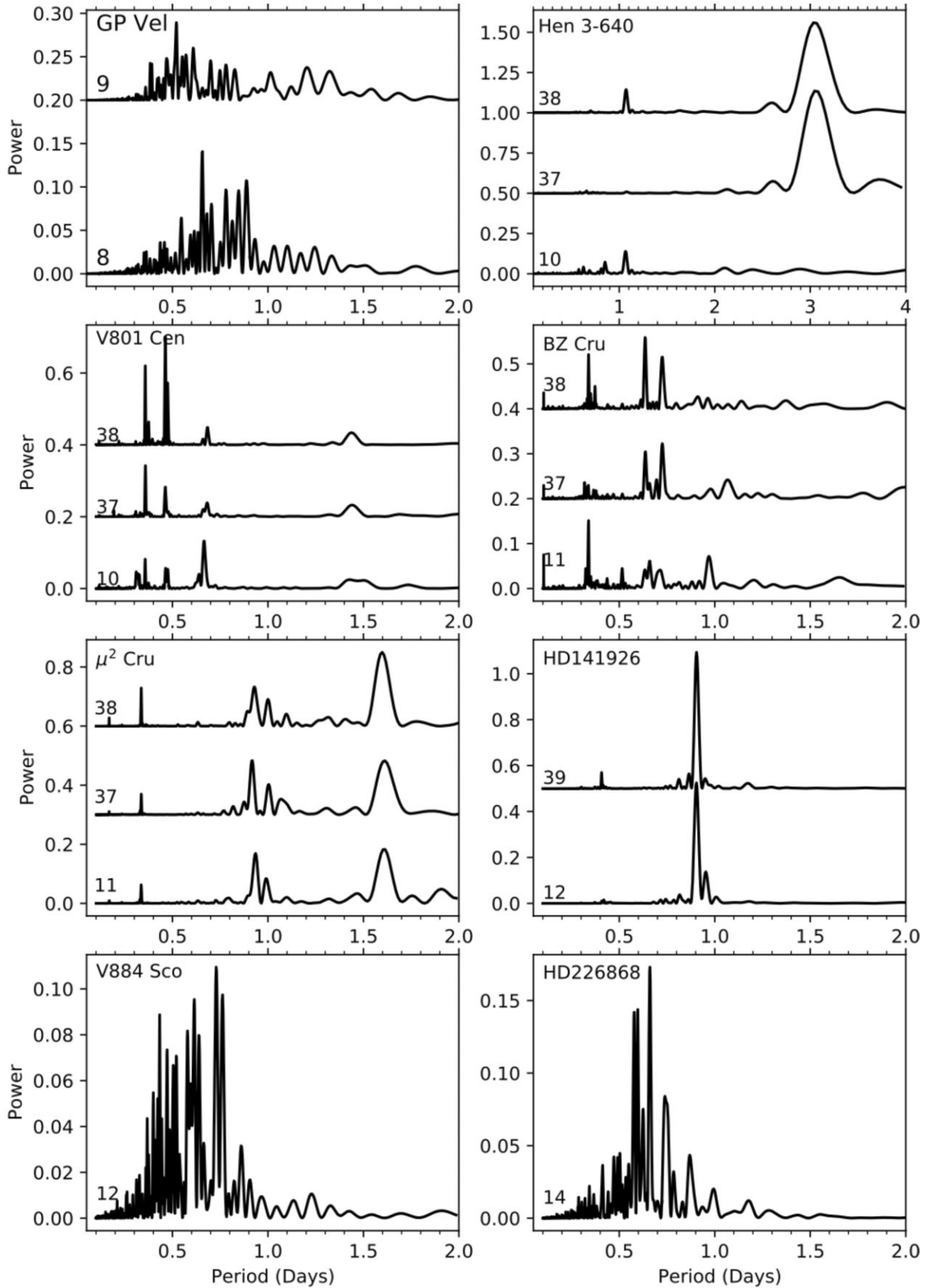
Figure 3. The LS power spectra of the *TESS* light curves of our HMXB sample, each labelled with the sector where the data originated.
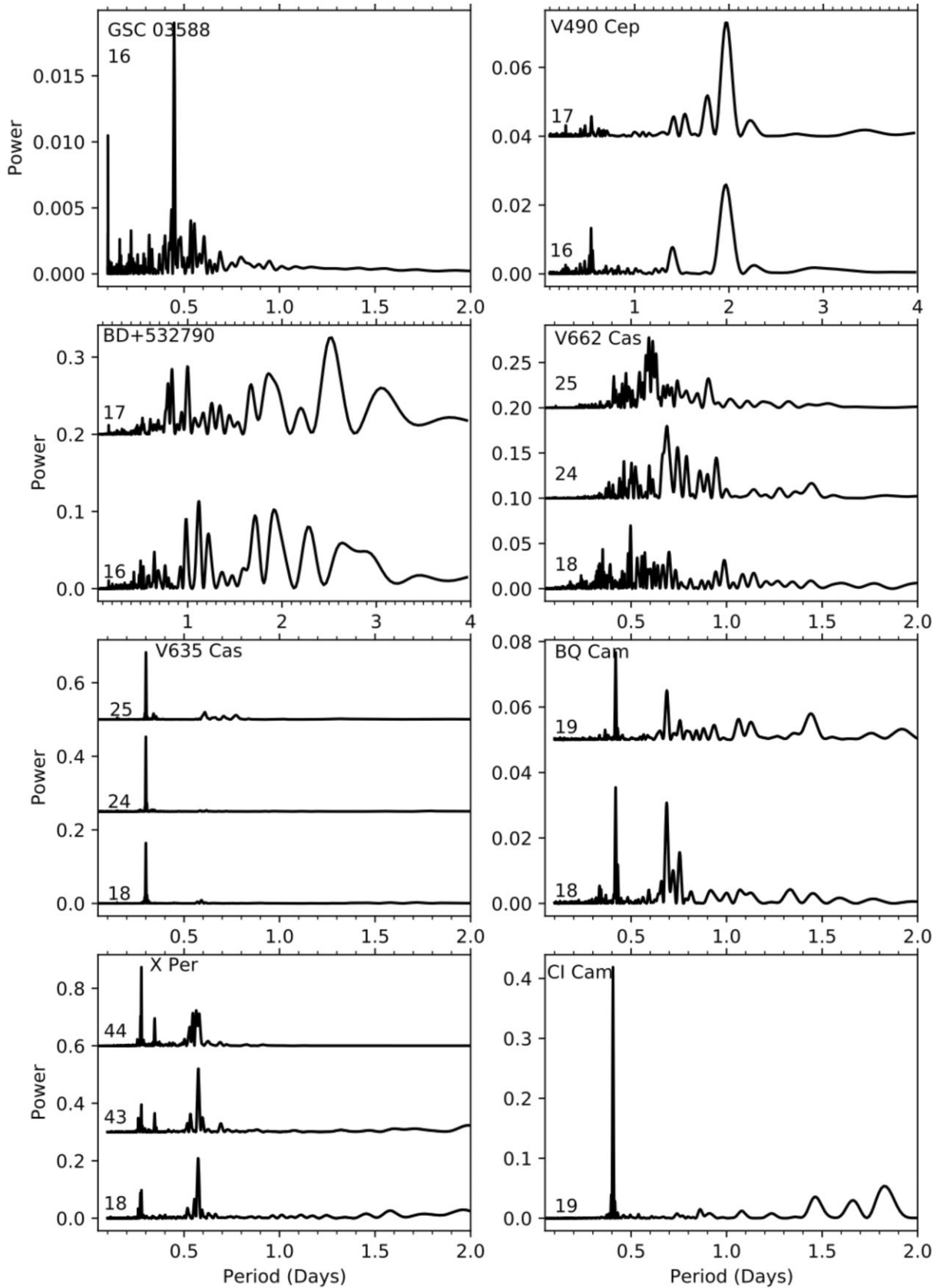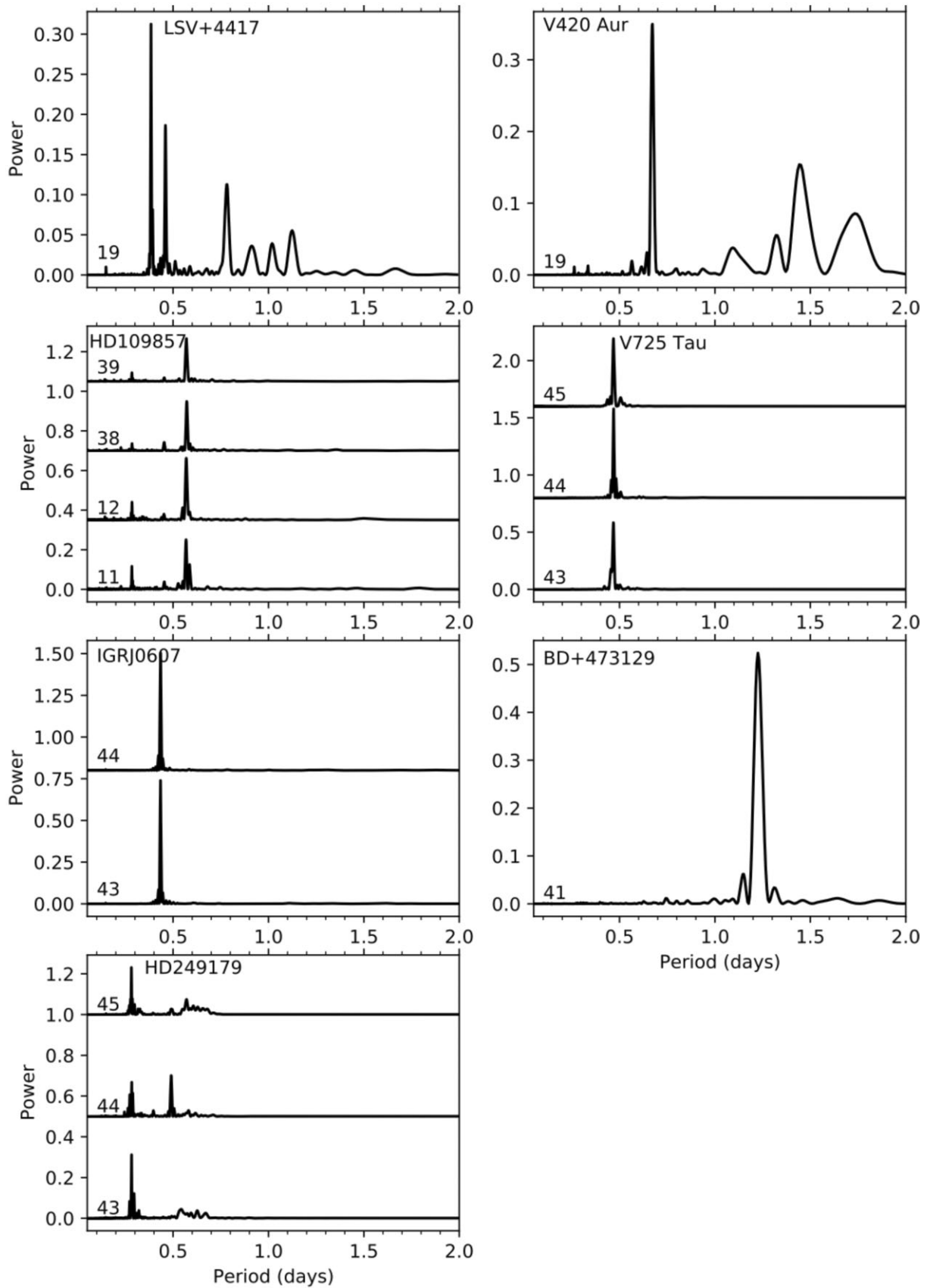
Figure 4. Fig. 3 continued.
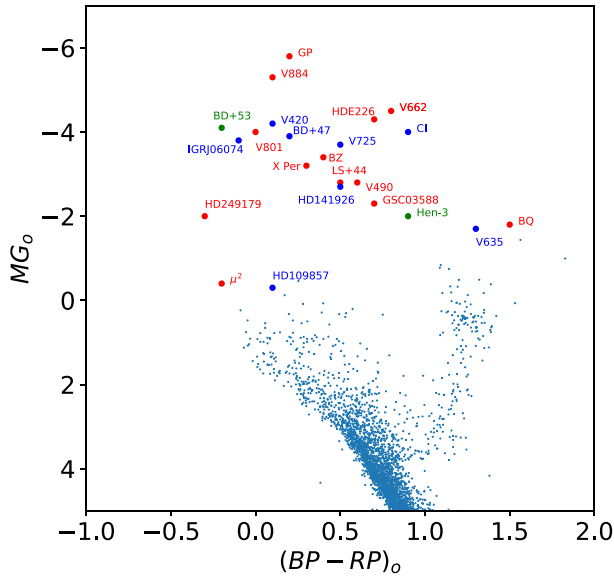
Figure 5. Fig. 4 continued.

Figure 6. The *Gaia* HRD as shown in Fig. 1 but here with the colour of the symbol representing those sources with mid-frequency signals in red, isolated signals in blue, and those showing mid- and low-frequency signals in green.

evolution of the pulsations over the *TESS* observations. First, long-term variations were removed, after which we moved a 2 d wide time window in steps of 0.05 d through the observations and carried out the epoch folding analysis with 30 phase bins for each step. We show the resulting trailed periodogram in the upper left-hand panel of Fig. 7. There is no apparent change in the amplitude of the $\sim$0.5 d period during or immediately after the optical outburst. However, it is clear that we detect at least three epochs of increased pulsation amplitude, separated by $\sim$30 d. An analysis of variance periodogram (Schwarzenberg-Czerny 1996) using the full detrended light curve finds a peak in the power spectrum at 13.6 d: This is half of the reported period of $\sim$28 d determined using radial velocities (Hutchings et al. 1978). Given the orbital period is 111 d, it is unclear what the origin of the 28 d period is due to.

4.2 HD 249179

4U 0548+29 (Forman et al. 1978) was associated with the B5ne star HD 249179 by Wackerling (1970) and classed as an HMXB in the catalogue of Liu et al. (2006). However, Torrejón & Orr (2001) made pointed observations of HD 249179 using *BeppoSAX* and found no evidence for X-ray emission, concluding that HD 249179 was not in fact the optical counterpart of 4U 0548+29. Nevertheless, we have retained HD 249179 in this study as a potential HMXB, since Be stars are known to undergo long intervals of weak or no X-ray emission, as a result of their highly eccentric orbits (Okazaki & Negueruela 2001).

In Fig. 7 (right-hand panels), we show the light curve of HD 249179 during sector 45: In the second half, after a slight decline in flux, there is a rapid increase of $\sim$0.1 mag (this increases to $\sim$0.14 mag once dilution from nearby bright stars is taken into account). We believe this is the first recorded optical outburst from HD 249179.

The detrended light curve of HD 249179 (Fig. C2) shows a quasi-periodic signal on a period of $\sim$0.28 d. This light curve also highlights how the amplitude of the short-period modulation increases by a factor of $\sim$3 at the same time as the start of the optical outburst. This is also demonstrated in the sliding epoch folding periodogram shown

in the upper right-hand panel of Fig. 7. In addition, there is some evidence that after the peak of the outburst has been reached, most of the power is transferred from the initial 0.28 d period to twice that (i.e. from 3.6 to 1.7 d^{-1} in frequency). We speculate that material has been ejected from this Be star to its disc.

5 DISCUSSION

We now discuss pulsations from isolated early-type stars and previous observations of outbursts from Be-type stars.

5.1 Pulsations from early-type stars

Bowman (2020) gives an overview of observations of high-mass stars, including β Cep and SPB stars. *TESS* observations of nearly 100 OB stars, coupled with high-resolution optical spectroscopy, were presented by Burssens et al. (2020), who found that many of them showed pulsations and concluded that if the modes of pulsation could be determined, then asteroseismic modelling would be possible. They identified a group of pulsators that show periods of a few days, such as SPBs that were likely due to coherent g-mode pulsations. Furthermore, β Cep stars show periods of a few tenths of a day, which are likely due to coherent p-mode pulsations. In addition, there are a group of stars that appear to be hybrid pulsators, showing both g- and p-mode pulsations. Sharma et al. (2022) presented *TESS* observations of 119 B-type stars that were members of the Sco–Cen association and found pulsations in 2/3 of the stars they sampled. Although they initially applied a cut-off at 0.4 d where stars were likely to be SPB if the main periods were <0.4 d and β Cep if >0.4 d, they conclude that it was not always possible to separate these stars purely on this criterion. Indeed, there were stars that appeared to be hybrids showing power in both frequency ranges.

However, based on these criteria, we find that 42 per cent of our sample were hybrids, 33 per cent were SPBs, and 25 per cent were β Cep stars. This compares with 23 per cent hybrids, 28 per cent SPBs, and 40 per cent β Cep stars as we have estimated from table 1 of Sharma et al. (2022). Given the indirect nature of the comparison, and that the Sharma et al. (2022) study covers all B spectral sub-types, while our sample is more concentrated on earlier sub-types or even giant/sub-giants, there is not a large difference in the fractions of types in these two studies.

5.2 Outbursts

Optical outbursts have been seen from many Be stars with time-scales ranging from days, weeks to years (e.g. Labadie-Bartz et al. 2018). The outburst causes material to be expelled from the star and forms (or maintains) an *excretion* disc. Much of this material eventually returns on to the star (see Rivinius et al. 2013 for details).

Using *TESS* observations, we have detected optical outbursts from V725 Tau and HD 249179. V725 Tau is a *bona fide* HMXB with an NS as it primary. In contrast, there is some doubt that HD 249179 is an HMXB, but rather an isolated Be star (Torrejón & Orr 2001). The outburst from V725 Tau showed no change in the period or amplitude of the short-period modulation, which is likely due to p-mode oscillations in the donor star. In contrast, we have found evidence that the period changes slightly during the outburst of HD 249179, with strong evidence that the amplitude increases significantly at the time where the outburst starts.

The outburst that we detected in HD 249179 is very similar to the outburst seen in HD 49330 (B0.5IVe) made using *CoRoT* data (Huat et al. 2009). They found that the amplitudes of the p modes
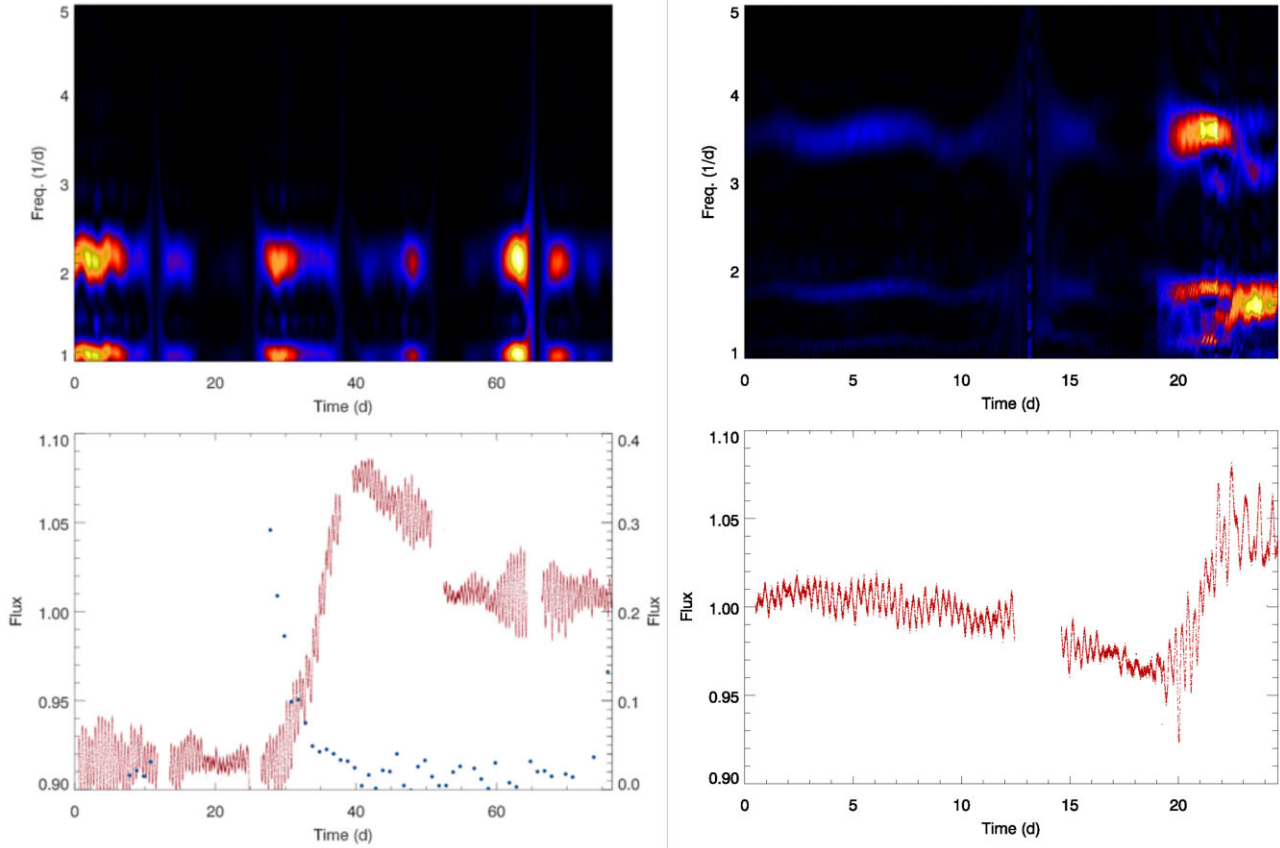
Figure 7. Lower panels: an outburst of V725 Tau (left-hand panel), which started on 2021 October 13 (day zero corresponds to MJD = 59473.68) during *TESS* sector 44, together with the MAXI X-ray data (blue dots). The right-hand panel shows an outburst of HD 249179 during *TESS* sector 45 (day zero corresponds to MJD = 59525.54). Upper panels: sliding periodograms of the *TESS* light curves (V725 Tau, left-hand panel, HD 249179, right-hand panel) where the colour intensity is scaled to reflect the amplitude of the power.

(short period) and g modes (long period) were directly correlated with the outburst: The amplitude of the p modes decreased just before the outburst and increased after the start of outburst. This is almost identical to our findings for HD 249179. Indeed, there is evidence that the combination of pulsation modes actually causes outbursts from Be stars (e.g. Baade et al. 2017), with the increase in the amplitude of the pulsations during the outburst being explained by stochastically excited waves (e.g. Baade et al. 2018; Neiner et al. 2020). More detailed work would be needed to identify the modes in HD 249179 before a similar study could be undertaken on the *TESS* outburst data.

It is not clear whether HD 249179 is a binary system. Unfortunately, there are no radial velocity data for it in *Gaia* DR3, presumably since it is in the Galactic plane ($b = 1.9°$) where blending of the Radial Velocity Spectrograph (RVS) spectra can be a serious issue. Studies on the multiplicity of early-type stars (see Sana 2017 for an overview) suggest that the multiplicity fraction of B4–9-type stars in the Milky Way is ∼1/5. It is therefore a matter of speculation of whether the outburst seen in HD 249179 is due to tidal interaction of a companion star.

6 CONCLUSIONS

We have shown that each of the 23 optical counterparts to the HMXBs in this survey shows clear evidence of quasi-periodic modulations with periods in the range ∼0.1–1 d, which fully supports the earlier

ground-based observations of HMXBs by Gutierrez-Soto et al. (2011) and Schmidtke et al. (2014, 2016, 2019). Many other massive stars, including Be stars, also show quasi-periodic pulsations with similar periods. To be able to derive fundamental parameters of the stars, it is essential to identify the modes in the power spectrum. This is not normally achievable just from broad-band photometry, but generally must be combined with high-resolution spectra (e.g. Aerts et al. 2019). However, this will be much more difficult to achieve for HMXBs where an accretion disc will make it difficult to separate the disc and stellar pulsation emission. Observations of massive eclipsing binaries (e.g. Southworth et al. 2020) show that tidal forces can affect the pulsation frequencies. Given that some HMXBs, primarily those with Be donor stars, have a non-negligible eccentricity (e.g. Vela X-1 has $e \sim 0.09$), it is possible that a more detailed study of the pulsation spectrum as a function of their orbital period may reveal some dependence on the orbital phase. Finally, in Cycle 5, the cadence of *TESS* full-frame images will be 200 s, which will allow many more HMXBs and early-type stars to be searched for pulsations.

DATA AVAILABILITY

The *TESS* data are available from the NASA MAST portal (https://archive.stsci.edu/) and MAXI data are available from the Riken MAXI portal (http://maxi.riken.jp).

REFERENCES

Aerts C. et al., 2019, A&A, 624, A75
Andrae R. et al., 2018, A&A, 616, A8
Astraatmadja T. L., Bailer-Jones C. A. L., 2016, ApJ, 833, 119
Baade D. et al., 2017, in Zwintz K., Poretti E., eds, Proc. Polish Astron. Soc., vol. 5, Second BRITE-Constellation Science Conference: Small Satellites – Big Science. Polish Astron. Soc., Warsaw, p. 196
Baade D. et al., 2018, A&A, 610, A70
Bailer-Jones C. A. L., 2015, PASP, 127, 994
Borucki W. J. et al., 2010, Science, 327, 977
Bowman D. M., 2020, Front. Astron. Space Sci., 7, 70
Burssens S. et al., 2020, A&A, 639, A81
Caldwell D. A., 2020, Res. Notes Am. Astron. Soc., 4, 201
Court J. M. C. et al., 2019, MNRAS, 488, 4149
Davies S. R., 1990, MNRAS, 244, 93
De Cat P., Uytterhoeven K., Gutiérrez-Soto J., Degroote P., Simón-Díaz S., 2011, in Neiner C., Wade G., Meynet G., Peters G., eds, Proc. IAU Symp., vol. 272, Active OB Stars: Structure, Evolution, Mass Loss, and Critical Limits. Cambridge, p. 433
Fausnaugh M. M. et al., 2021, ApJ, 908, 51
Forman W., Jones C., Cominsky L., Julien P., Murray S., Peters G., Tananbaum H., Giacconi R., 1978, ApJS, 38, 357
Foster G., 1996, AJ, 112, 1709
Gaia Collaboration 2018, A&A, 616, A1
Gaia Collaboration, 2021, A&A, 649, A1
Gerend D., Boynton P. E., 1976, ApJ, 209, 562
Green G. M. et al., 2019, ApJ, 887, 93
Gutierrez-Soto J., Reig P., Fabregat J., Fox-Machado L., 2011, in Neiner C., Wade G., Meynet G., Peters G., eds, Proc IAU Symp., vol. 272, Active OB Stars: Structure, Evolution, Mass Loss, and Critical Limits. Cambridge, p. 505

Hakala P., Ramsay G., Barclay T., Charles P., 2015, MNRAS, 453, L6
Hall T. A., Finley J. P., Corbet R. H. D., Thomas R. C., 2000, ApJ, 536, 450
Huat A.-L. et al., 2009, A&A, 506, 95
Hutchings J. B., Bernard J. E., Crampton D., Cowley A. P., 1978, ApJ, 223, 530
Hynes R. I. et al., 2016, MNRAS, 459, 3596
Kong L. D. et al., 2021, ApJ, 917, L38
Labadie-Bartz J. et al., 2018, AJ, 155, 53
Labadie-Bartz J., Carciofi A. C., de Amorim T. H., Rubio A., Luiz A., Ticiani dos Santos P., Thomson-Paressant K., 2022, AJ, 163, 226
Lewin W. H. G., van der Klis M., eds, 2006, Compact Stellar X-ray Sources. Cambridge Univ. Press, Cambridge
Lightkurve Collaboration, 2018, Astrophysics Source Code Library, record ascl:1812.013
Liu Q. Z., van Paradijs J., van den Heuvel E. P. J., 2006, A&A, 455, 1165
Neiner C., Lee C., Mathis S., Saio H., Lovekin C. C., Auguston K. C., 2020, A&A, 644, A9
Okazaki A. T., Negueruela I., 2001, A&A, 377, 160
Press W. H., Teukolsky S. A., Vetterling W. T., Flannery B. P., 1992, Numerical Recipes in C, 2nd edn., Cambridge Univ. Press, New York
Ricker G. et al., 2015, J. Astron. Telesc. Instrum. Syst., 1, 014003
Rivinius T., Carciofi A C., Martayan C., 2013, A&AR, 21, 69
Sana H., 2017, in Eldridge J. J., Bray J. C., McClelland L. A. S., Xiao L., eds, Proc. IAU Symp., vol. 329, The Lives and Death-Throes of Massive Stars. Cambridge, p. 110
Scaringi S. et al., 2015, MNRAS, 451, 3857
Schmidtke P. C., Cowley A. P., Udalski A., 2014, Astron. Telegram, 5781
Schmidtke P. C., Cowley A. P., Udalski A., 2016, Astron. Telegram, 9320
Schmidtke P. C., Cowley A. P., Udalski A., 2019, Astron. Telegram, 13128
Schwarzenberg-Czerny A., 1996, ApJ, 460, L107
Sharma A. N., Bedding T. R., Saio H., White T. M., 2022, MNRAS, 515, 828
Southworth J., Bowman D. M., Tkachenko A., Pavlovski K., 2020, MNRAS, 497, L19
Taylor M. B., 2006, in Gabriel C., Arviset C., Ponz D., Solano E., eds, ASP Conf. Ser., vol. 351, Astronomical Data Analysis Software and Systems XV. Astron. Soc. Pac., San Francisco, p. 666
Torrejón J. M., Orr A., 2001, A&A, 377, 148
Vieira S. L. A., Corradi W. J. B., Alencar S. H. P., Mendes L. T. S., Torres C. A. O., Quast G. R., Guimarães M. M., da Silva L., 2003, ApJ, 126, 2971
Wackerling L. R., 1970, MNRAS, 73, 153
Zechmeister M., Kürster M., 2009, A&A, 496, 577

APPENDIX A: LIGHT CURVES

The light curves of all the HMXBs in our sample where we indicate in each panel the *TESS* sector the data originated. For most cases, we show the first sector of data where more than one sector of data was obtained.
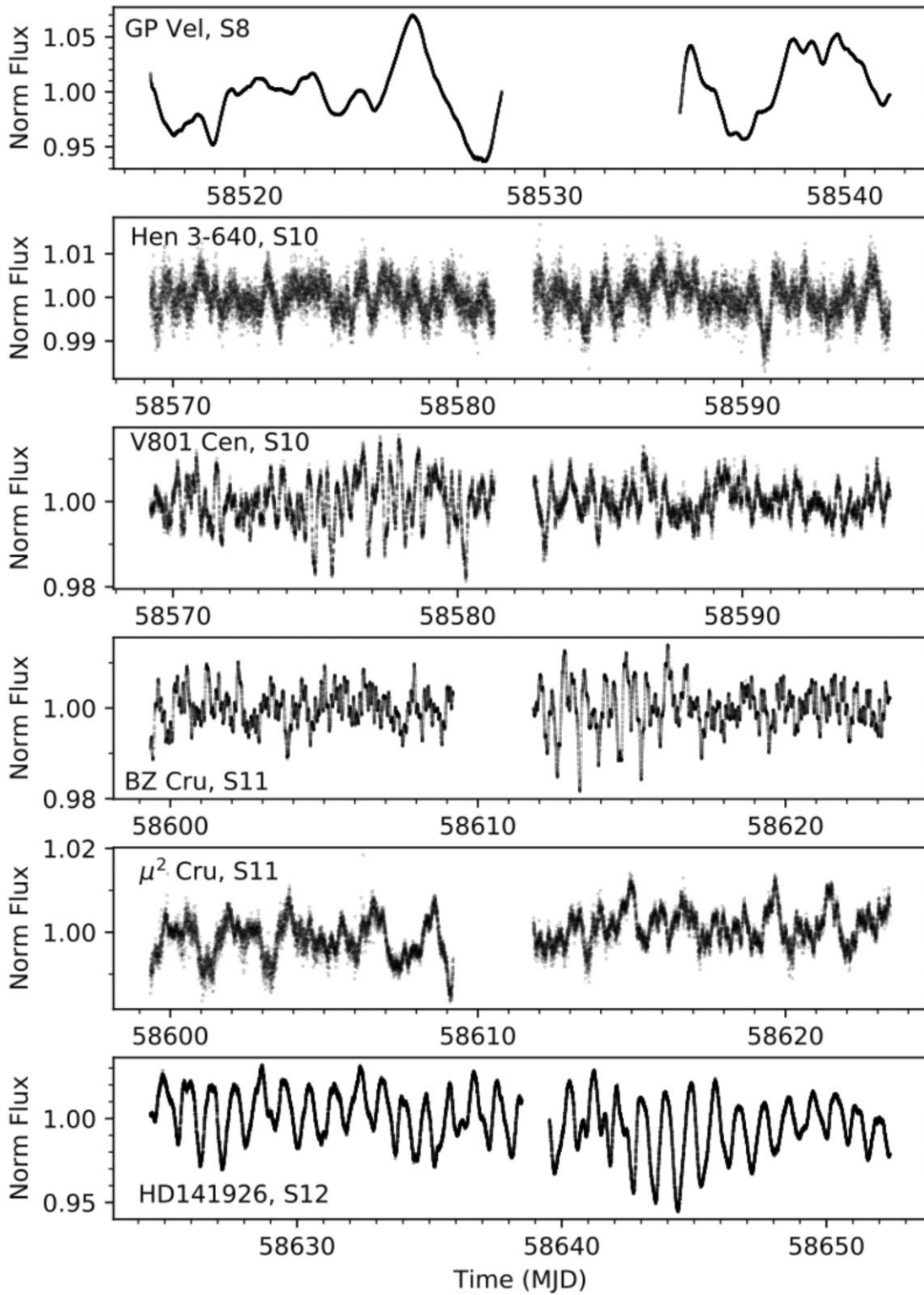
Figure A1. The *TESS* light curves of the HMXBs in our sample where we indicate which sector the data originated.
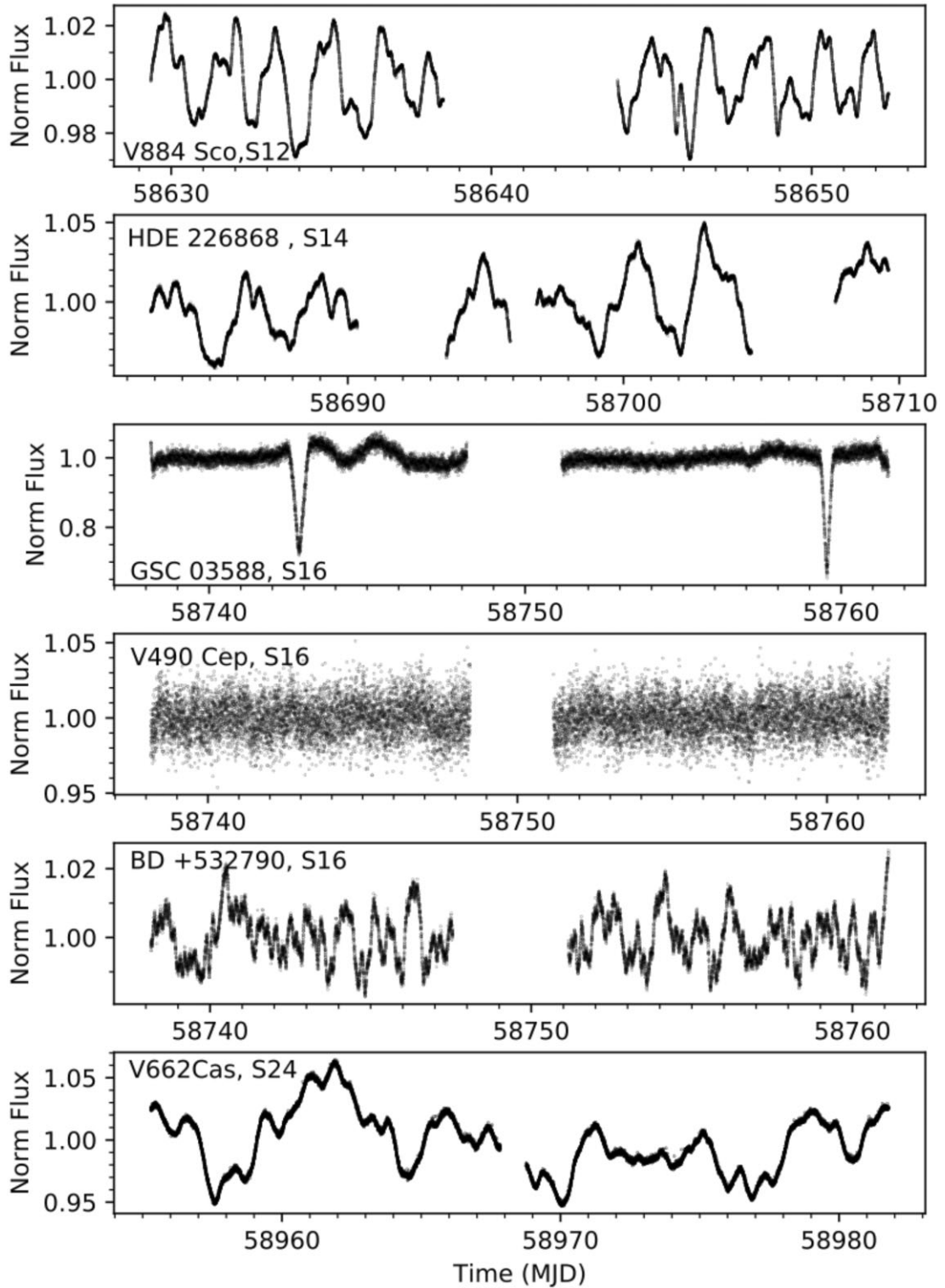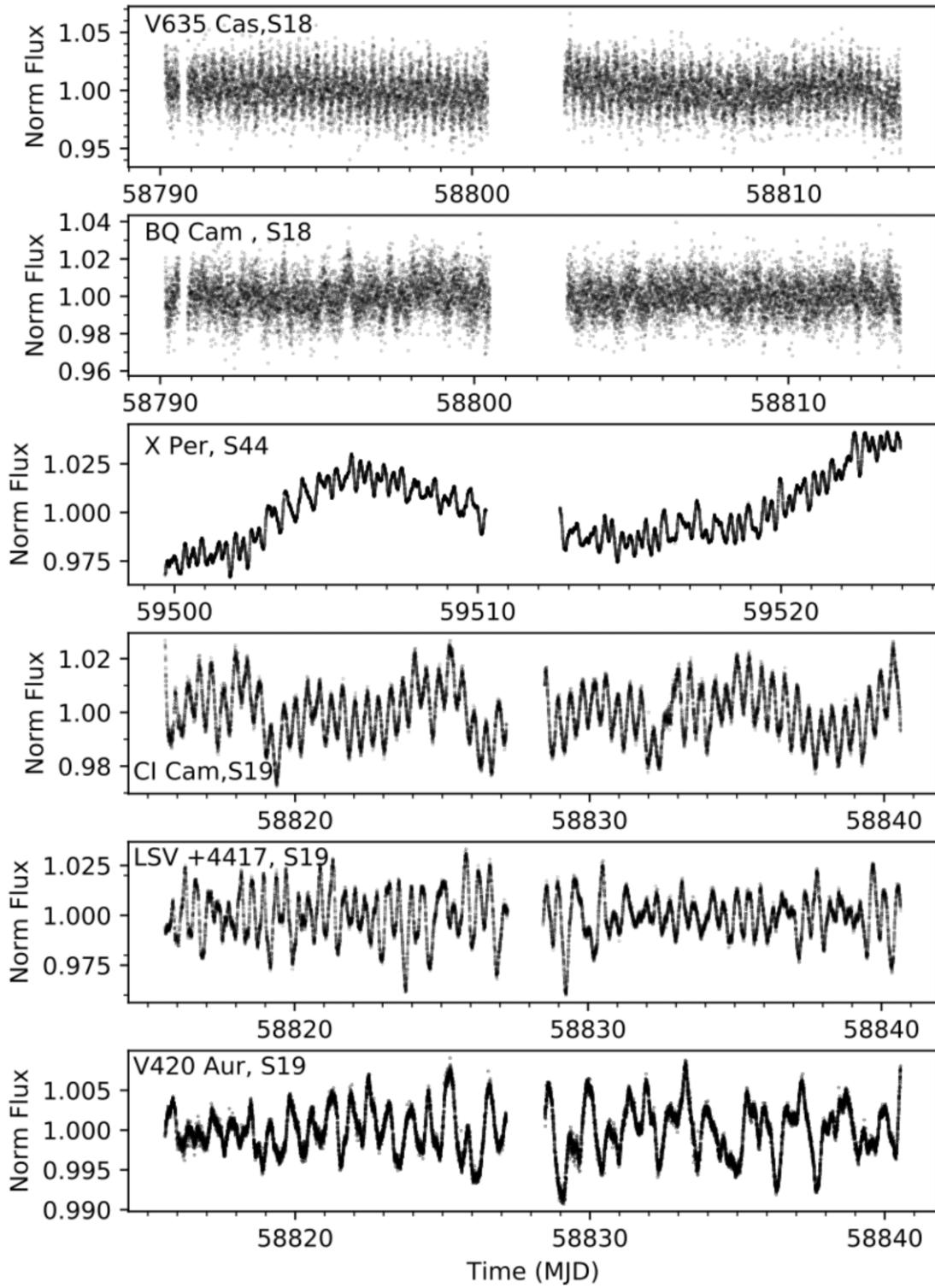
Figure A2. Fig. A1 continued.

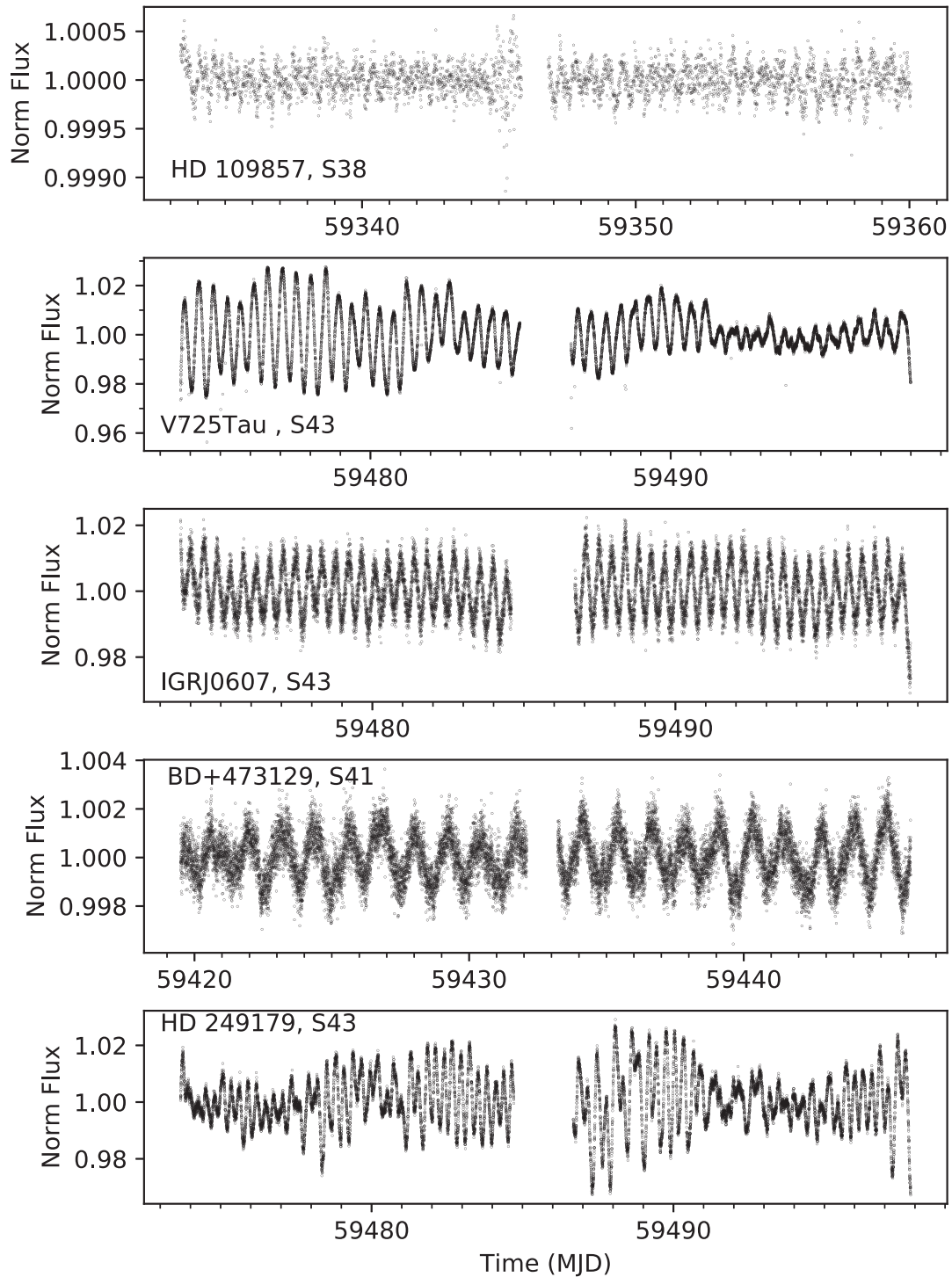**Figure A3.** Fig. A2 continued.

Figure A4. Fig. A3 continued.

APPENDIX B: DETRENDED LIGHT CURVES

For sources showing high-amplitude variations in their light curve over the orbital period we detrended the signature of the orbital period to search for short-period pulsations. In Fig. 2, we show the original and detrended light curve of HDE 226868 (Cyg X-1). Here, we show the original and detrended light curves of GP Vel, V884 Sco, and V662 Cas.
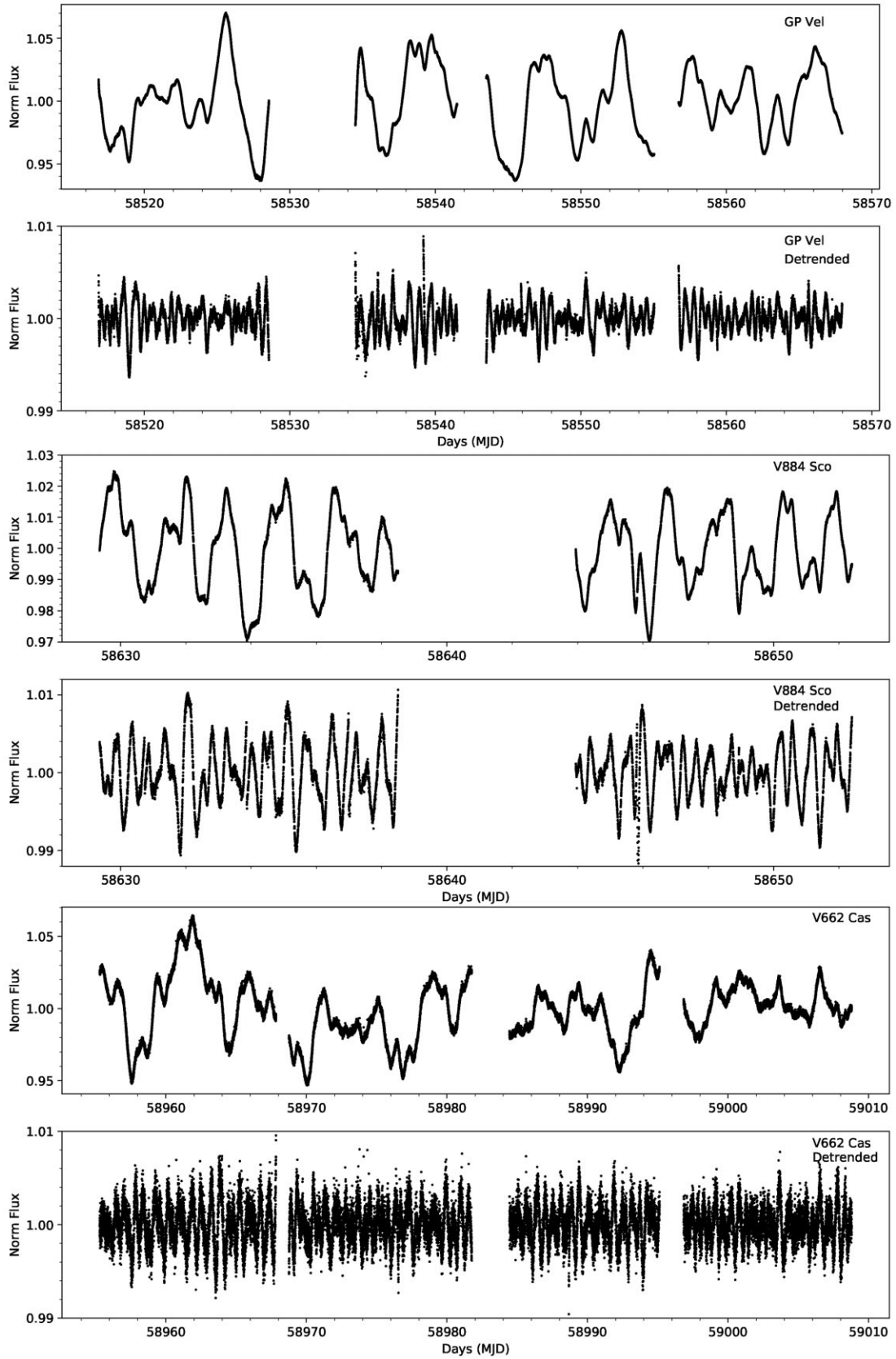
Figure B1. The original and detrended light curves of GP Vel, V884 Sco, and V662 Cas.

APPENDIX C: LIGHT CURVES

The light curves of V725 Tau and HD 249179 that have been detrended to remove the signature of the outburst. The time of the optical outbursts is indicated for each source.
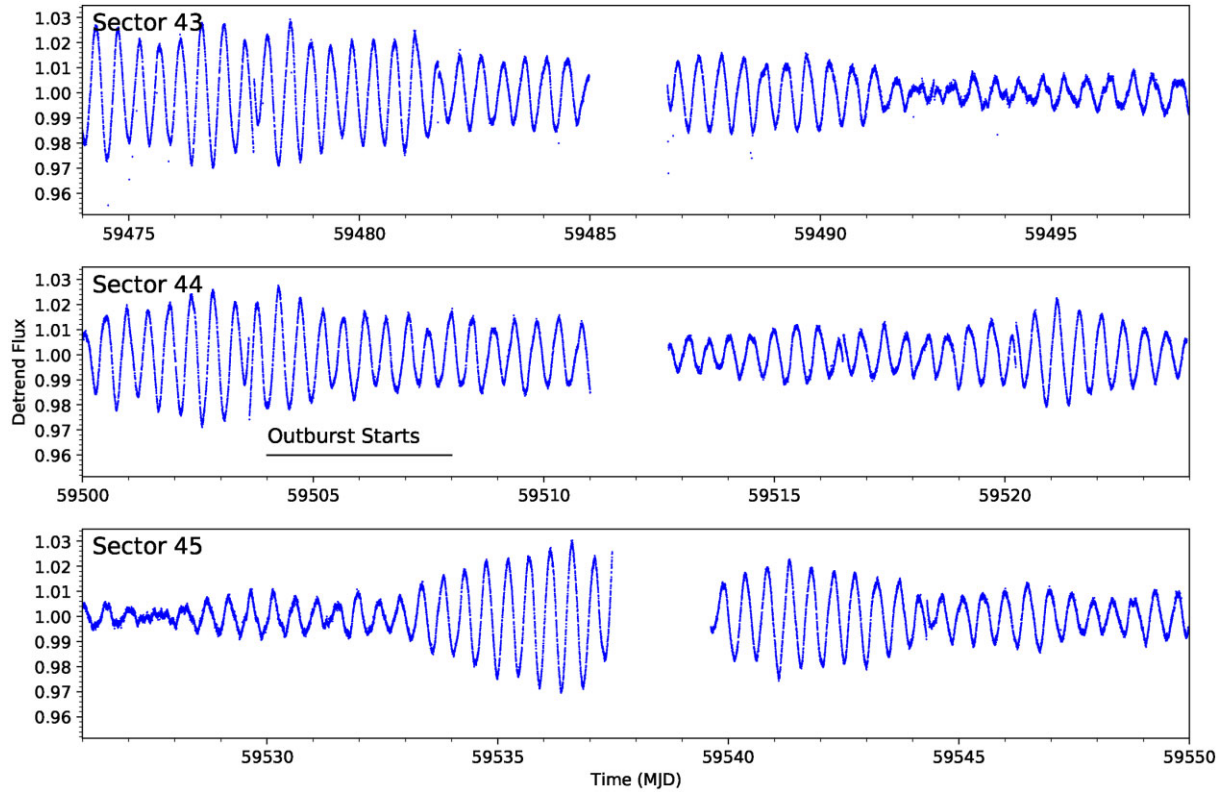

Figure C1. The *TESS* light curve of V725 Tau, which has been detrended to remove the outburst and long-term variations. The resulting curve has a prominent signal at ∼0.48 d.
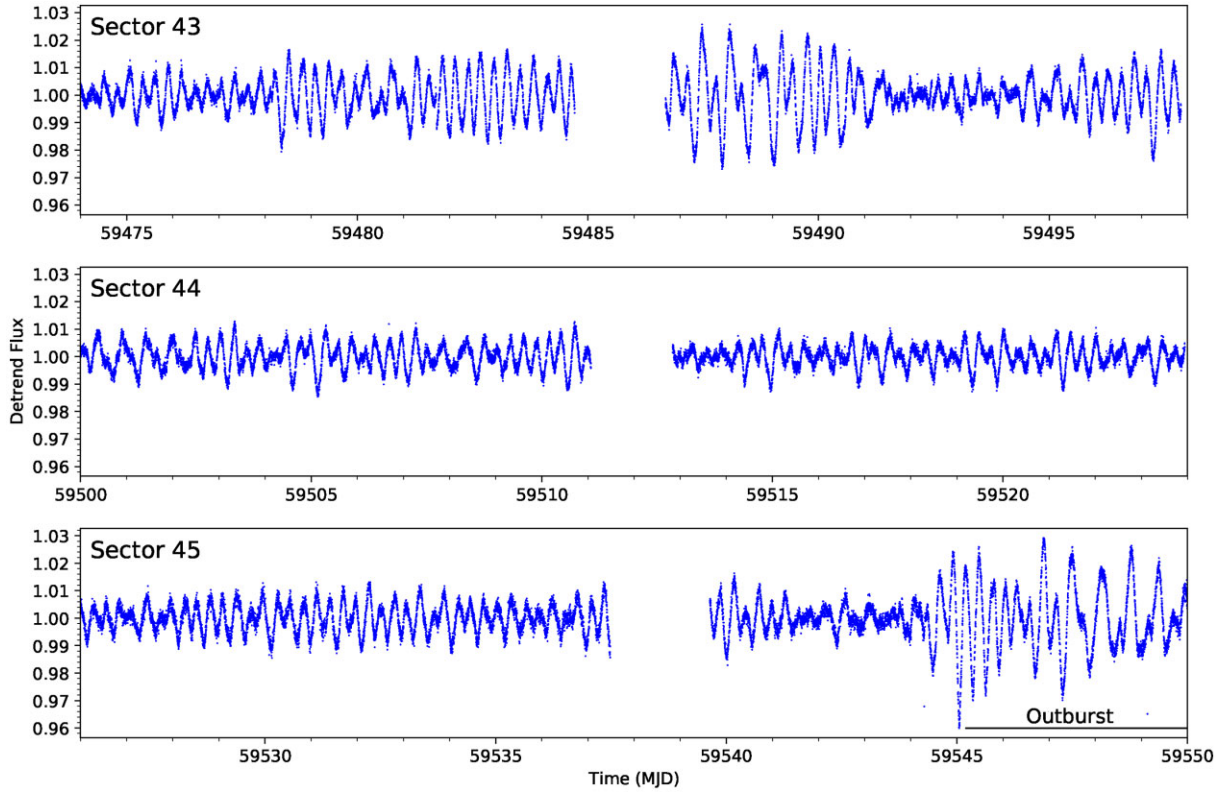
Figure C2. The *TESS* light curve of HD 249179, which has been detrended to remove the outburst and long-term variations. The resulting curve has a prominent signal at ~0.28 d.

This paper has been typeset from a TEX/LATEX file prepared by the author.